Pulsatile blood flow in human bone assessed by laser-Doppler flowmetry and the interpretation of photoplethysmographic signals

2013 Physiol. Meas. 34 N25

(http://iopscience.iop.org/0967-3334/34/3/N25)

Physiol. Meas. **34** (2013) N25–N40 doi:10.1088/0967-3334/34/3/N25

NOTE

Pulsatile blood flow in human bone assessed by laser-Doppler flowmetry and the interpretation of photoplethysmographic signals

Tiziano Binzoni[1,2], David Tchernin[2], Jean-Noël Hyacinthe[2], Dimitri Van De Ville[2,3] and Jonas Richiardi[2,3]

[1] Département de Neurosciences Fondamentales, University of Geneva, Geneva, Switzerland
[2] Département de l'Imagerie et des Sciences de l'Information Médicale, University Hospital, Geneva, Switzerland
[3] Institute of Bioengineering, Ecole Polytechnique Fédérale de Lausanne (EPFL), Lausanne, Switzerland

E-mail: tiziano.binzoni@unige.ch

Received 25 October 2012, accepted for publication 7 February 2013
Published 26 February 2013
Online at stacks.iop.org/PM/34/N25

Abstract
Human bone blood flow, mean blood speed and the number of moving red blood cells were assessed (in arbitrary units), as a function of time, during one cardiac cycle. The measurements were obtained non-invasively on five volunteers by laser-Doppler flowmetry at large interoptode spacing. The investigated bones included: patella, clavicle, tibial diaphysis and tibial malleolus. As hypothesized, we found that in all bones the number of moving cells remains constant during cardiac cycles. Therefore, we concluded that the pulsatile nature of blood flow must be completely determined by the mean blood speed and not by changes in blood volume (vessels dilation). Based on these results, it is finally demonstrated using a mathematical model (derived from the radiative transport theory) that photoplethysmographic (PPG) pulsations observed by others in the literature, cannot be generated by oscillations in blood oxygen saturation, which is physiologically linked to blood speed. In fact, possible oxygen saturation changes during pulsations decrease the amplitude of PPG pulsations due to specific features of the PPG light source. It is shown that a variation in blood oxygen saturation of 3% may induce a negative change of $\sim$1% in the PPG signal. It is concluded that PPG pulsations are determined by periodic 'positive' changes of the reduced scattering coefficient of the tissue and/or the absorption coefficient at constant blood volume. No explicit experimental PPG measurements have been performed. As a by-product of this study, an estimation of the arterial pulse wave velocity obtained from the analysis of the blood flow pulsations give a value of 7.8 m s^{-1} (95% confidence interval of the sample mean distribution: [6.7, 9.5] m s^{-1}), which is perfectly compatible with data in the literature. We hope that this note will contribute to

a better understanding of PPG signals and to further develop the domain of the vascular physiology of human bone.

Keywords: pulse wave velocity, tibial diaphysis, tibial malleolus, patella, clavicle, non-invasive, radiative transport theory, mean blood speed

(Some figures may appear in colour only in the online journal)

1. Introduction

Bone and its vascular and nervous system represent an indissociable triad for the good functioning of the human skeletal system. Better understanding the mechanisms underlying the interaction between these systems appears to be a fundamental point considering the potential clinical impact. In this context, the development of non-invasive techniques allowing continuous monitoring of blood flow directly in human bone is a mandatory topic to be addressed.

Unfortunately, the nature of bone itself makes it exceptionally difficult to study blood circulation continuously, non-invasively or over long and repeated periods of time. Investigations on short-time intervals revealing, for example, the pulsatile nature of blood flow, also remain a technical challenge. Measurement techniques that are usually applied in the laboratory are difficult or impossible to apply on humans, and when applicable they are partially invasive and allow only a few measurements in time (Brookes and Revell 1998). Attracted by the technical challenge, some years ago, our group started to investigate the possibility of using near-infrared light as a new probe to monitor blood-flow-related parameters in human bone (Binzoni *et al* 2002, 2003a, 2006, 2011, Binzoni and Van De Ville 2011). Since then other groups successfully used near-infrared light and found different solutions to directly or indirectly estimate bone blood flow (Näslund *et al* 2006, 2007, Aziz *et al* 2010, Mateus and Hargens 2012).

Interestingly enough, the latter series of studies have shown the possibility to *indirectly* monitor blood flow 'pulsations' in the human patella (Näslund *et al* 2006, 2007). This technical problem was solved by the authors by using a classical photoplethysmography (PPG) technique (Challoner 1979, Roberts 1982, Allen 2007) at 804 nm wavelength. As it is well known, PPG allows the detection of tissue blood volume changes, through the change of the wavelength-dependent (λ) tissue optical absorption coefficient ($\mu_a(\lambda)$), and thus indirectly blood flow pulsations. However, patellar bone has a structure that is considered rigid and vessels should in principle not dilate during the systolic time-intervals. To explain this point, Näslund *et al* (2006) hypothesized that PPG pulsations were induced by a change in shape and orientation of the red blood cells due to the periodic increase in mean blood flow speed. This hypothesis was corroborated by previous *in vitro* observations on rigid glass tubes (Challoner 1979, Lindberg and Öberg 1993) where the blood speed and flow, but not the volume, can change. In these papers, the intensity of the detected light (PPG signal) was changing as a function of blood speed with constant blood volume. The difficult task was to understand by which physical phenomenon this could happen.

One possible mechanism was related to the change in the reduced scattering ($\mu'_{sb}(\lambda)$) and absorption ($\mu_{ab}(\lambda)$) coefficients of blood induced by the red blood cell deformation and change in orientation occurring during blood flow pulsations (Roggan *et al* 1999, Friebel *et al* 2007).

It was found that both $\mu'_{sb}(\lambda)$ and $\mu_{ab}(\lambda)$ decrease for increasing blood speed. However, from the point of view of PPG this is an astonishing result, because a decrease in $\mu'_{sb}(\lambda)$ or $\mu_{ab}(\lambda)$, as a function of increasing speed, means a decrease in the PPG signal and not an increase (positive pulse) as observed *in vivo* (see section 4.1.3)[4]. This may be due to the fact that $\mu'_{sb}(\lambda)$ and $\mu_{ab}(\lambda)$ have been measured on plasma-free blood samples, an *in vitro* model far from the real biological conditions. Moreover, real bone morphology is not equivalent to a single relatively large glass tube. In real bone a huge number of red blood cells (average diameter 7.8 μm) are continuously deforming, when passing through capillaries (diameter 3–7 μm) (Dobbe *et al* 2002), independent of the blood speed. Cells pass through a dense and intricate vascular network where the vessels' diameters go from very large to very small relative to their size. This means that red blood cells may have an infinite variety of different shapes, continuously varying in time, with a multitude of orientations. This is why *in vivo* fluid dynamics of the whole blood (non-Newtonian fluid) is extremely different from that in a single tube and thus may influence $\mu'_{sb}(\lambda)$ and $\mu_{ab}(\lambda)$ in a different manner than *in vitro*. Note that *in vivo*, it is not enough to consider only $\mu'_{sb}(\lambda)$ or $\mu_{ab}(\lambda)$, because the PPG signal actually depends on the *total* reduced scattering coefficient $\mu'_s(\lambda)$ and $\mu_a(\lambda)$ of the tissue, where the contribution of $\mu'_{sb}(\lambda)$ and $\mu_{ab}(\lambda)$ to $\mu'_s(\lambda)$ and $\mu_a(\lambda)$ represent only a fraction of these values.

It is clear from the above observations that it is extremely difficult to forecast, even with sophisticated numerical simulations, if and how $\mu'_s(\lambda)$ and/or $\mu_a(\lambda)$ vary at each pulsation (Mishchenko *et al* 2000) at constant blood volume. Moreover, the above discussion may also cast a doubt on the validity of the constant 'blood volume' hypothesis for real bone. The *in vivo* establishment of the behaviour of $\mu'_s(\lambda)$ or $\mu_a(\lambda)$ during heart beats is an unsolved issue, and the explanation of the PPG pulsations observed in bone remains an open question.

For all the above reasons, in the present contribution the human bone blood volume is experimentally measured during a cardiac pulsation and the hypothesis of constant blood volume is explicitly tested. The validity (or not) of this hypothesis implies completely different interpretations when explaining $\mu'_s(\lambda)$ and/or $\mu_a(\lambda)$ variations in bone. Then, by means of a mathematical model, it is shown what must finally be the direction of variation of $\mu'_s(\lambda)$ and/or $\mu_a(\lambda)$ if one wants to observe a positive PPG pulsation, as it is the case for real *in vivo* measurements.

More precisely, the experimental part of this note comprehend: (1) the *direct* and non-invasive measurement of the pulsatile bone blood flow (Φ); (2) checking blood volume remains constant during blood pulsations, by measuring the number of moving red blood cells ($\bar{n}$); (3) the assessment of the mean blood flow speed (V). The measurements of Φ, $\bar{n}$ and V, are performed by laser-Doppler flowmetry (LDF) at large interoptode spacing and are assessed from the zero- ($\langle\omega^{(0)}\rangle$) and first-order ($\langle\omega^{(1)}\rangle$) moment (in arbitrary units) of the power density spectrum ($P(\omega)$) of the measured photo-electric current ($i(t)$):

$$\bar{n} \propto \langle\omega^{(0)}\rangle / i_0^2, \tag{1}$$

$$\Phi \propto \langle\omega^{(1)}\rangle / i_0^2, \tag{2}$$

$$V \propto \Phi / \bar{n}, \tag{3}$$

where

$$i_0 := \lim_{T\to+\infty} \frac{1}{2T} \int_{-T}^{T} \mathrm{i}(t)\,\mathrm{d}t, \tag{4}$$

[4] By convention, in PPG an upward deflection of the signal indicates a decrease in the intensity of the detected light (Lindberg and Öberg 1991).

and

$$\langle \omega^{(n)} \rangle := \int_{-\infty}^{\infty} |\omega|^n \, P(\omega) \, \mathrm{d}\omega, \tag{5}$$

($n \in \{0, 1\}$), with

$$P(\omega) := \left| \int_{-\infty}^{\infty} \mathrm{i}(t) \, \mathrm{e}^{-\mathrm{i}\omega t} \, \mathrm{d}t \right|^2, \tag{6}$$

and $\omega = 2\pi\nu$ the angular frequency (Binzoni *et al* 2003b, 2011).

By taking into account the obtained experimental results, the theoretical part is developed through a well-known analytical model derived from the radiative transport theory. The influence of an increase/decrease of $\mu_s'(\lambda)$ and/or $\mu_a(\lambda)$ on the PPG signal is clearly derived. For the sake of completeness, the possible influence of tissue blood oxygen saturation ($\%SO_2$) is also investigated.

As a by-product of this work, it is shown that LDF allows the assessment of the classical pulse wave velocity of blood (with the difference that the detector here is at bone level), which is a fundamental parameter for clinical investigations of the arterial system (Nichols *et al* 2011). This last possibility might allow one day for the study of blood pulse wave propagation in human bone.

In conclusion, the capability to monitor blood flow pulsations in human bone might open new domains of research and clinical applications, related for example to the fine and non-invasive study of the role of the autonomic nervous system in the control of bone/bone marrow blood perfusion (Binzoni and Van De Ville 2011).

2. Material and methods

2.1. ECG-triggered laser-Doppler flowmeter

The present set of measurements has been realized with a previously described (Binzoni *et al* 2003b, 2011) LDF at large interoptode spacing ($r = 1.5$ cm). The measured parameters, expressed in arbitrary units, were: V, $\bar{n}$ and $\Phi = V\bar{n}$.

Changes in V, $\bar{n}$ and Φ values occurring during one heart cycle were monitored by triggering the LDF with an electrocardiograph (ECG). The ECG R-peaks were hardware-detected by the LDF system. At each detected R-peak a trigger signal was generated and the LDF started to acquire 24 values for each parameter V, $\bar{n}$ and Φ. The sampling time for the 24 acquisitions was 32.8 ms. To increase the signal-to-noise ratio, the above operation was repeated 200 times (i.e. for 200 trigger R-peaks). This allowed us to obtain mean V, $\bar{n}$ and Φ, and relative confidence intervals. The measured values (24×3) were stored on a hard disk for further analysis. In figure 1, we schematically summarize the acquisition procedure.

2.2. Experimental protocol

The illustrative non-invasive measurements were performed on five healthy male subjects, the authors, aged 38.2 ± 9.5 years, body mass 75.0 ± 6.3 kg, stature 181.6 ± 5.4 cm. The subject was comfortably seated in a room at $\sim$24 $^{\circ}$C and was wearing comfortable clothing allowing to easily access the different investigated bones.

A portable ECG (CARDIOLAB4, Francesco Marazza, Hardware & software, Monza, Italy) was connected to the investigated subject and its analogue output connected to the LDF (see section 2.1).

The LDF optical probe was placed consecutively on four different measurement positions (see figure 2): (1) on the right patella, centred along the midsagittal line; (2) on the right tibial

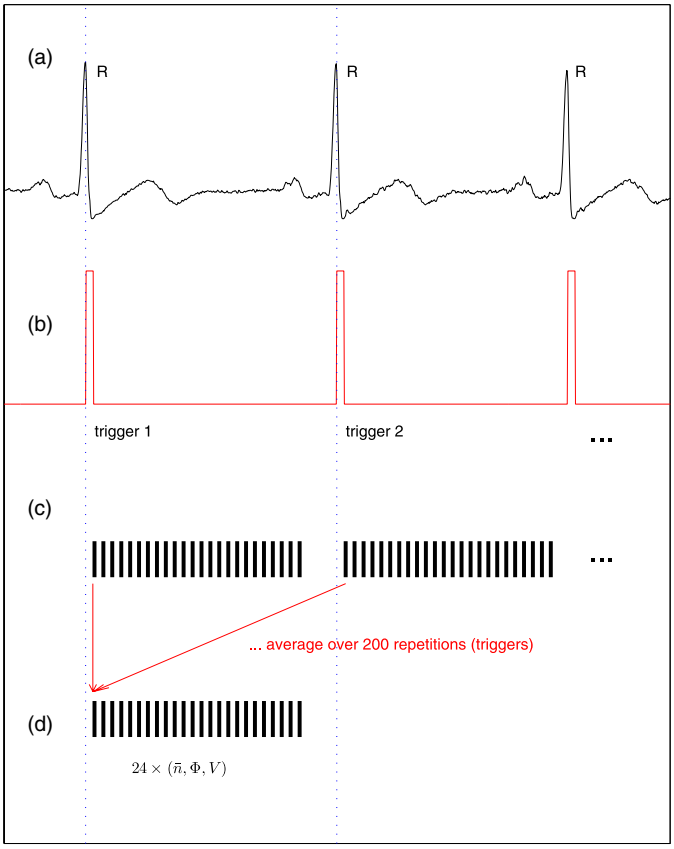

Figure 1. Schematic of the acquisition procedure adopted to assess the bone mean blood speed (V), the number of moving red blood cells ($\bar{n}$) and the mean blood perfusion (Φ) during a heart pulse cycle. At each R-peak of the ECG (a) a trigger signal (b) is generated. At each trigger signal, the acquisition of 24 values for each of the parameters V, $\bar{n}$ and Φ is started (c). This procedure is repeated for 200 triggers. Since the acquisition of the V, $\bar{n}$ and Φ are synchronized with the ECG, their mean values can be computed (d).

diaphysis, on the medial surface of the tibia, at the half distance between the medial malleolus and the medial condyle; (3) on the right medial malleolus of the tibia, with the probe oriented at 45° (clockwise) from the coronal plane passing through the malleoulus; (4) on the right clavicle, at the junction of its lateral and middle third. For each subject, this resulted into four different sets of measurements for V, $\bar{n}$ and Φ. The LDF optical probe was slightly pressed against the skin surface to eliminate possible skin or periosteal blood flow. In fact, pushing an optode against the bone cortex with a force of ∼77 g is enough to generate a pressure of ∼200 mm Hg (larger than the systolic pressure) under the probe, which is sufficient to stop the blood flow. A schematic drawing representing a general LDF optical probe is reported in figure 3. Note that a PPG optical probe having the same interoptode distance, r, and geometrical configuration as that of LDF, 'observe' the same tissue region of interest (ROI).

The distance (L) between the hydrostatic arterial reference point (intersection of the midaxillary line with the horizontal plane through the upper border of the fourth chondromanubrial junction; see figure 2) and the four LDF positions was also measured

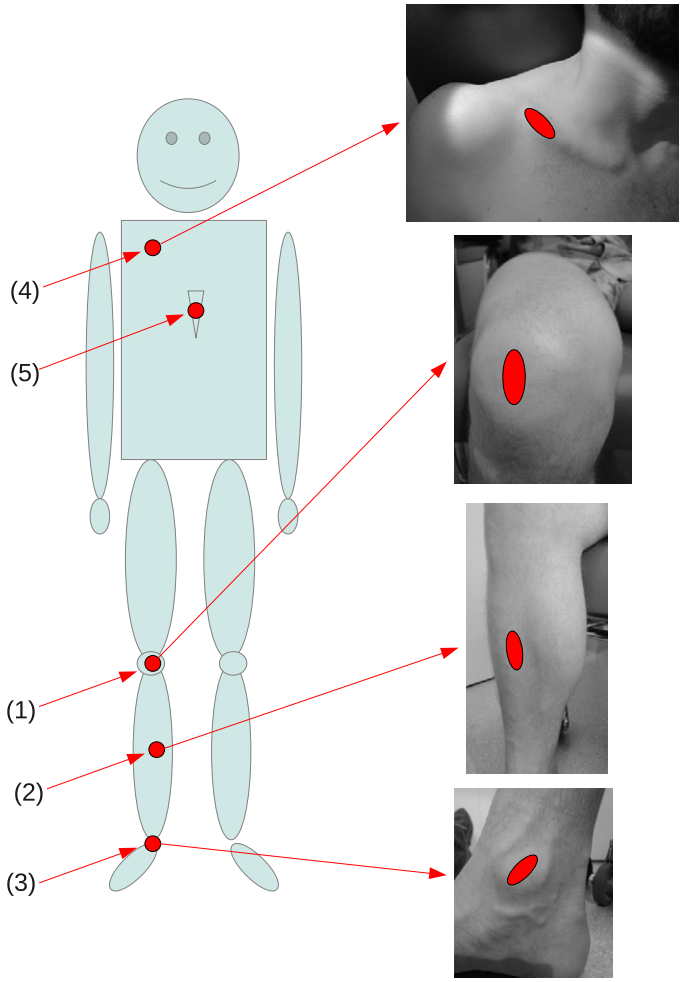

Figure 2. (1), (2), (3) and (4): positions of the LDF optodes (see section 2.2); (5) hydrostatic arterial reference point.

on each subject by means of a ruler. These values have been utilized as a rough approximation of the length of the vascular path going from the left heart to the LDF measurement point.

3. Results

In figure 4, $\bar{n}$, Φ and V are shown as a function of time (t) for a typical subject and for two representative bones: the patella and the clavicle. The confidence intervals appearing in the figure have been estimated by bootstrap using the bias corrected and accelerated percentile method (Di Ciccio and Efron 1996). This statistical method does not necessitate assumptions about the underlying probability distribution function of the data points. Considering that the confidence intervals are relative to the sample mean probability distribution, they allow to directly determine if two mean values on the graphs are significantly different.

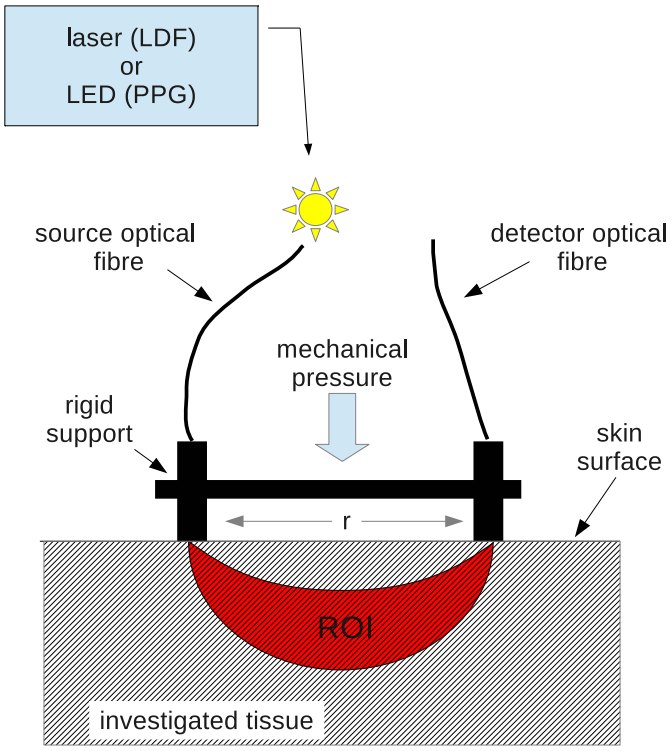

Figure 3. Schematic drawing showing a typical configuration for a representative laser-Doppler flowmeter (LDF) optical probe. Note that this configuration is similar to a representative photoplethysmographic (PPG) probe. For the same interoptode spacing (r), LDF and PPG techniques measure the same region of interest (ROI, represented by the red region). The light source for the LDF is a laser and for the PPG a light emitting diode (LED). In the case of the PPG the intensity of the detected light is analysed to obtain a parameter related to the tissue blood flow and blood volume. In the case of LDF the small changes in frequency observed on the detected light are analysed to obtain parameter-related tissue blood flow, mean blood speed and the number of moving red blood cells.

It has been demonstrated (Binzoni *et al* 2006) that blood volume can change in bone. However, these changes are slow, probably due to the absence of lymphatic vessels in normal bone (Edwards *et al* 2008), and cannot occur periodically during heart pulsations. In fact, to increase the bone blood volume, an equivalent volume of interstitial fluid (situated outside the vessels) must be displaced from the interstitial tissue surrounding the vessels. Otherwise, a bone 'dilation' would be necessary, which is not a phenomenon that may occur in a few tens of milliseconds. To confirm this point, in the present contribution the blood volume has been assessed by LDF by observing the changes in the number of moving red blood cells ($\bar{n}$; proportional to changes in blood volume). It appears from figure 4 that $\bar{n}$ remains constant and thus, as hypothesized, blood volume does not change during heart pulsations. This experimentally confirms the hypothesis that in bone there is no significant periodic increase in blood volume due to vasodilation or opening of collaterals (Näslund *et al* 2006). From this observation it follows that the pulsatile character of Φ can only be determined by the periodic variations in V.

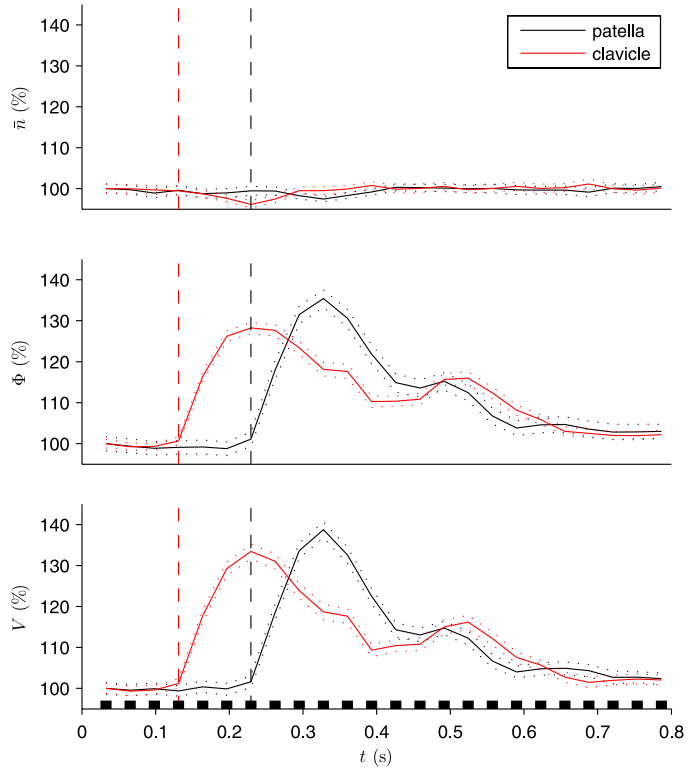

Figure 4. The number of moving red blood cells ($\bar{n}$), mean blood perfusion (Φ) and mean blood speed (V) values for a typical subject as a function of time (t), measured at the patella (black lines) and at the clavicle (red lines). The cardiac cycle duration is ∼1 s. The vertical red and black dashed lines represent the arrival time of the pulse wave and is defined as Δt in this note. The black ticks on the abscissa represent the times when $\bar{n}$, Φ and V have been sampled. The dotted red and black lines are the 95% confidence intervals of the sample mean probability distribution. Ordinate axes start at a value of 95%.

From figure 4 we can also observe that Φ and V tracings contain minor maxima, appearing at ∼0.52 s (clavicle and patella) or at ∼0.35 (clavicle only). Considering the timing of appearance, this secondary maxima might be assimilated to well-known mechanical events (e.g., closure of cardiac valves), linked to the cardiac contraction cycle, and also observed on radial artery pressure wave recordings (Nichols *et al* 2011). This observation, deserves further investigation in the future.

Another interesting observation is that Φ and V pulsations do not start exactly at $t = 0$ (beginning of the cardiac systole), but they display a clear delay (Δt). In fact, the pulse wave generated by the cardiac contraction needs some time to reach the point of measurement. This explains why this wave arrives before in the clavicle and then the patella (situated at a larger distance, L, from the right ventricle compared to the clavicle). Considering that each measurement position is situated at different distances from the heart, and that the anatomical characteristics of each subject are different due to the different statures, Δt should vary accordingly. The measured ranges in the subjects of L for the medial malleolus of the tibia, the patella, the clavicle and the tibial diaphysis were [112, 129], [71, 88], [21, 24] and [90, 107] cm, respectively.

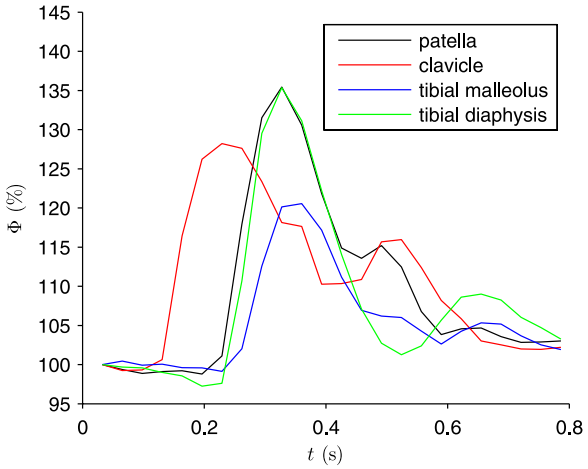

Figure 5. Mean blood perfusion (Φ) as a function of time (t) measured at four different bone positions, for a typical subject.

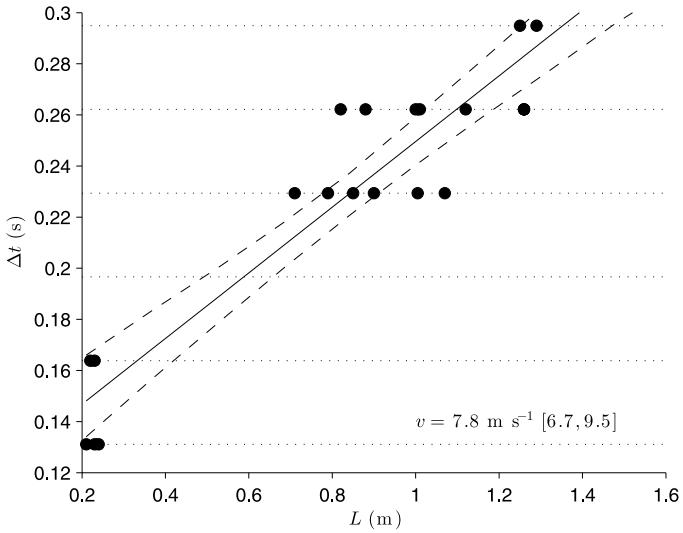

Figure 6. Time delay (Δt; see also figure 4) as a function of the distance, L, travelled by the blood from the left ventricle to the LDF measurement point. Measurements performed on five subjects and four different measurement points, resulting in $5 \times 4 = 20$ experimental data (black circles). The continuous line is the estimated regression line. Dashed lines represent the 95% confidence intervals of the probability distribution of the abscissa statistic. Values in the square parenthesis define the 95% confidence intervals of the sample mean probability distribution for v.

In figure 5 the Φ pulses as a function of t for all the bone positions are shown for a typical subject.

Figure 6 reports the Δt values as a function of L (see section 2.2). Due to the finite time resolution of the present LDF system, Δt is discretized, which corresponds to the horizontal dotted lines in figure 6 (i.e. no Δt values can be measured experimentally between two dotted lines). By analysing the slopes obtained by linear-regression fitting to the experimental data

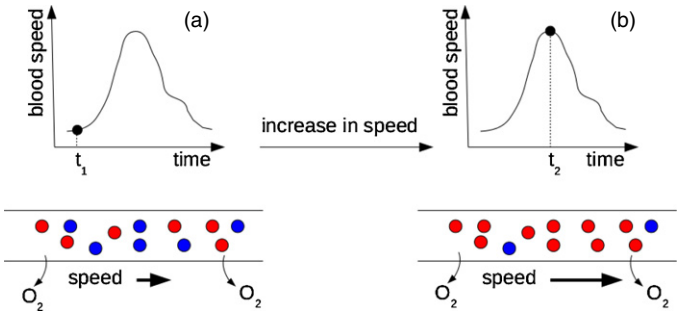

Figure 7. Schematic drawing showing the effect of an increase in blood speed on the haemoglobin oxygen saturation ($\%SO_2$). Red dots represent oxygenated haemoglobin molecules and blue deoxygenated ones. $\%SO_2$ is the ratio of the number of red dots to the total number of dots (red plus blue). The horizontal 'tubes' in panels (a) and (b) represent a typical capillary observed at time t_1 and t_2. If the blood speed increases (going from t_1 to t_2) then the oxygen extraction decreases (i.e. less time to extract oxygen from oxygenated haemoglobin) and by definition $\%SO_2$ increases. Note that the oxygen consumption remains constant along the time.

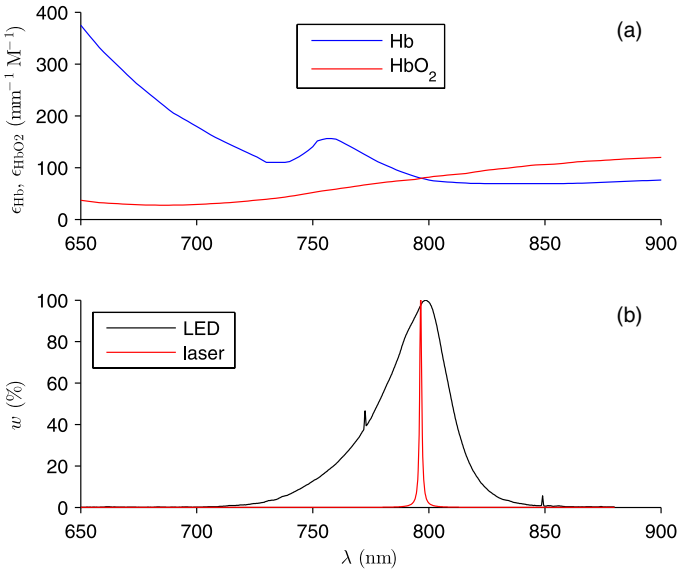

Figure 8. (a) Molar extinction coefficients as a function of wavelength (λ) for oxy- ($\epsilon_{HbO_2}(\lambda)$) and deoxy-haemoglobin ($\epsilon_{Hb}(\lambda)$). These data were downloaded from the Oregon Medical Laser Center web site http://omlc.ogi.edu. (b) Relative spectral emission ($w(\lambda)$) for a typical LED (black line) utilized in photoplethysmography (real data for a FQR5401 LED, Fietje Sensor&Optoelektronik GmbH, Germany). The red line reproduces the typical (theoretical) Lorentzian shape of the relative spectral emission of a laser (laser wavelength chosen at the isosbestic point). Scale on the abscissa is the same for (a) and (b).

points, it is possible to estimate the mean (globally for all the subjects together) speed (v) of the pulse wave. We found $v = 7.8$ m s^{-1}, falling in the range of values observed for the propagation of the pulse pressure wave velocity in the peripheral arteries (Solà *et al* 2010, Nichols *et al* 2011)[5]. The confidence intervals appearing in figure 6 have been estimated by

[5] Note that the pulse wave velocity is not the blood velocity. For example, the pulse wave velocity in a rigid tube is theoretically infinite, but the blood velocity remains finite.

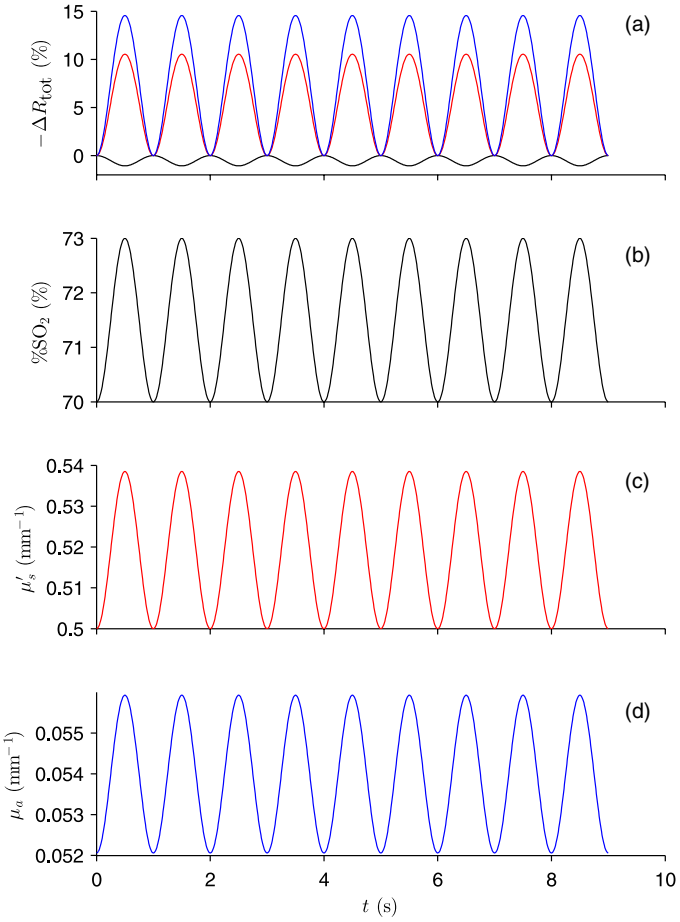

Figure 9. Results from the numerical simulation. Per cent changes of the photoplethysmographic signal ($\Delta R_{\rm tot}(\rho)$) as a function of time (t, panel (a)) in the presence of tissue blood oxygen saturation (%SO_2) oscillations (panel (b)). In panel (a) the black and red curves represent $\Delta R_{\rm tot}(\rho)$ when the photoplethysmograph source is a LED and a laser (see figure 8(b)), respectively. The abscissa scales are in common.

bootstrap using the bias corrected and accelerated percentile method (Di Ciccio and Efron 1996).

4. Discussion and conclusions

In the present contribution we have shown that, together with the measurement of V and $\bar{n}$, it is possible to monitor the pulsatile behaviour of Φ during one cardiac cycle, by LDF at large interoptode spacing. It has been found that in human bone Φ pulsations are determined by the changes in V at constant $\bar{n}$, which demonstrates the previous hypothesis of Näslund *et al* (2006). Thus, V pulsations appear to be possibly responsible for $\mu_{\rm s}'(\lambda)$ and/or $\mu_{\rm a}(\lambda)$ variations, and consequently for the PPG pulsations. As explained in the introduction section, changes in $\mu_{\rm s}'(\lambda)$ and/or $\mu_{\rm a}(\lambda)$ are probably due to the change in shape and orientation of the red blood cells. The direction and magnitude of these changes as a function of V remains to

be investigated *in vivo*. However, it must also be noted that $\mu_a(\lambda)$ values may also depend on haemoglobin O_2 saturation ($\%SO_2$). A change in $\%SO_2$ may occur due to V variations inducing a modification in 'oxygen extraction' (see section 4.1.1).

Considering the present results and lack of clear experimental information (see the introduction section) concerning the behaviour of $\mu'_s(\lambda)$, $\mu_a(\lambda)$ and $\%SO_2$ *in vivo*, and their influence on the PPG signal, we will treat this problem with the help of a mathematical model in the following sections.

The possibility to estimate the Φ-pulse wave velocity in bone vessels by means of LDF or PPG will also be shortly discussed.

4.1. Photoplethysmographic signal and haemoglobin oxygen saturation

We explain why PPG may be sensitive to $\%SO_2$ variations, induced by the changes in V (see figure 4), even with a LED light source centred at the isosbestic point. More specifically, we want to investigate if periodic increases in $\%SO_2$ (if any, see below), at constant total haemoglobin and $\mu'_s(\lambda)$, can explain the observed periodic positive pulses in PPG.

4.1.1. The 'oxygen extraction': a classical key concept. It is well known from physiology textbooks that, when V increases, oxygen extraction decreases, and vice versa (Comroe 1977, West 1990). In other words, when blood speed is increased then the blood spends less time in the capillaries and the tissue has less time to extract oxygen from haemoglobin. At higher speed we observe more oxyhaemoglobin (for the same total haemoglobin) compared to a lower blood speed. Thus, an increase/decrease in V, with the linked decrease/increase in oxygen extraction, signifies by definition an increase/decrease in $\%SO_2$. This means that $\%SO_2$ variations may occur without a change in the total haemoglobin content (proportional to the blood volume and linked to $\bar{n}$ in figure 4), which is the case for bone. Figure 7 illustrates this phenomenon in a schematic manner.

4.1.2. The bandwidth of the light source and the molar extinction coefficients. The wavelength of the light source (LED) usually utilized in PPG at large source/detector spacing is often chosen to be near the isosbestic point for haemoglobin (i.e. around 800 nm, the λ value for which the $\epsilon_{HbO_2}(\lambda)$ and $\epsilon_{Hb}(\lambda)$ curves cross each other in figure 8(a)). This particular choice is made with the purpose to eliminate the possibility to detect a variation in $\%SO_2$ in presence of constant blood volume, as is the case for bone (in this case we would be obliged to introduce the now infirmed hypothesis of varying $\mu'_s(\lambda)$ to explain the PPG signal). However, it must be noted that contrary to a laser, a real LED has a relatively large bandwith (see figure 8(b)) and the choice of its wavelength only refers to the maximum of its spectrum. This means that in practice the concept of isosbestic point does not hold for the LED because too many wavelengths off from this point are contributing to the spectrum. This fact has the consequence that actually *a PPG is also sensitive to $\%SO_2$ changes*, at constant or varying blood volume, even if the LED central λ is chosen to be near the isosbestic point. To discuss this phenomenon in a more formal manner, we will reproduce the $\%SO_2$-sensitivity in the next section of the PPG by means of a well-tested analytical model utilized in biomedical optics (Farrell *et al* 1992).

4.1.3. The mathematical model. Consider a homogeneous semi-infinite medium representing the investigated biological tissue. Without loss of generality let us choose $\mu'_s(\lambda) = 0.5\ \text{mm}^{-1}$ for all the investigated λ. If the light source/detector separation is $\rho = 15$ mm then, for a given

λ, the detected intensity on the PPG, $R(\rho, \lambda)$, is proportional to (Farrell *et al* 1992):

$$R(\rho,\lambda) \propto w(\lambda)\frac{a'(\lambda)}{2\pi}\left\{z_0(\lambda)\left[\mu_{\text{eff}}(\lambda)+\frac{1}{r_1(\rho)}\right]\frac{\mathrm{e}^{-\mu_{\text{eff}}(\lambda)r_1(\rho)}}{r_1(\rho)^2} + [z_0(\lambda)+2z_{\text{b}}(\lambda)]\left[\mu_{\text{eff}}(\lambda)+\frac{1}{r_2(\rho)}\right]\frac{\mathrm{e}^{-\mu_{\text{eff}}(\lambda)r_2(\rho)}}{r_2(\rho)^2}\right\}, \tag{7}$$

with the different parameters defined as

$$\mu'_{\text{t}}(\lambda) := \mu_{\text{a}}(\lambda)+\mu'_{\text{s}}(\lambda), \tag{8}$$

$$a'(\lambda) := \mu'_{\text{s}}(\lambda)\mu'_{\text{t}}(\lambda)^{-1}, \tag{9}$$

$$z_0(\lambda) := \mu'_{\text{t}}(\lambda)^{-1}, \tag{10}$$

$$\mu_{\text{eff}}(\lambda) := [3\mu_{\text{a}}(\lambda)\mu'_{\text{t}}(\lambda)]^{\frac{1}{2}}, \tag{11}$$

$$z_{\text{b}}(\lambda) := \tfrac{2}{3}(1+R_{\text{eff}})(1-R_{\text{eff}})^{-1}\mu'_{\text{t}}(\lambda), \tag{12}$$

and where $R_{\text{eff}} = 0.493$ is derived from the relative indices of refraction for a tissue/air interface (Farrell *et al* 1992). The remaining parameters are defined as

$$r_1(\rho)^2 := [\rho^2+z_0(\lambda)^2]^{\frac{1}{2}}, \tag{13}$$

$$r_2(\rho)^2 := [\rho^2+(z_0(\lambda)+2z_{\text{b}}(\lambda))^2]^{\frac{1}{2}}. \tag{14}$$

The parameter $w(\lambda)$ represents the relative spectral emission of the considered light source expressed in per cent (see, e.g., figure 8(b)). Thus, if the light source contains a range of λ, then the PPG signal becomes

$$R_{\text{tot}}(\rho) = \int_0^\infty R(\rho,\lambda)\,\mathrm{d}\lambda \tag{15}$$

Using (15), we want now to simulate the influence of a series of small $\%SO_2$ oscillations (see figure 9(b)), at constant blood volume, on the PPG signal $R_{\text{tot}}(\rho)$. The instrument will be a typical PPG with a LED light source (figure 8(b)). To this aim $\mu_{\text{a}}(\lambda)$ can be written as

$$\mu_{\text{a}}(\lambda) = f_{\text{H}_2\text{O}}\mu_a^{\text{H}_2\text{O}}(\lambda) + f_{\text{blood}}\left[\left(1-\frac{\%\text{SO}_2}{100}\right)\mu_a^{\text{Hb}}(\lambda)+\frac{\%\text{SO}_2}{100}\mu_a^{\text{HbO}_2}(\lambda)\right], \tag{16}$$

where $f_{\text{H}_2\text{O}} = 0.7$ and $f_{\text{blood}} = 0.07$ are the volume fractions of water and total haemoglobin present in the simulated tissue, respectively. The absorption coefficients for deoxygenated ($\mu_a^{\text{Hb}}(\lambda)$) and oxygenated ($\mu_a^{\text{HbO}_2}(\lambda)$) blood are obtained from

$$\mu_a^{\text{Hb}}(\lambda) = \ln(10)c_{\text{hb}}M_{\text{w}}^{-1}\epsilon_{\text{Hb}}(\lambda), \tag{17}$$

$$\mu_a^{\text{HbO}_2}(\lambda) = \ln(10)c_{\text{hb}}M_{\text{w}}^{-1}\epsilon_{\text{HbO}_2}(\lambda), \tag{18}$$

where $c_{\text{hb}} = 150$ g l^{-1} and $M_{\text{w}} = 64\,000$ g mole^{-1} are the concentration of haemoglobin in blood and the gram molecular weight of haemoglobin, respectively. Note that in this context we consider only the main and obvious influence of $\%SO_2$ on $\mu_{\text{a}}(\lambda)$. Varying the parameters $\mu'_{\text{s}}(\lambda)$, $f_{\text{H}_2\text{O}}$, f_{blood} and c_{hb} in the physiological range for different tissues gives similar results and does not change the purposes and the main conclusions of the present simulation.

Thus, by inserting in the previous equations the pulsating $\%SO_2$ values appearing in figure 9(b), one can calculate $R_{\text{tot}}(\rho)$ as a function of t. In figure 9(a) are shown the relative $R_{\text{tot}}(\rho)$ percentage changes compared to its value at $t = 0$:

$$\Delta R_{\text{tot}}(\rho) = \frac{R_{\text{tot}}(\rho)-R_{\text{tot}}(\rho)|_{t=0}}{R_{\text{tot}}(\rho)|_{t=0}}100. \tag{19}$$

Note that the minus sign in figure 9(a), $-\Delta R_{\mathrm{tot}}(\rho)$, is due to the fact that the PPG signal is reported with an opposite sign compared to the detected light intensity. From figure 9 one can see that a small oscillation of 3% in $\%SO_2$ can induce a change of $\sim$1% in the PPG signal $-R_{\mathrm{tot}}(\rho)$. This result is compatible with previous experimental observations where $\%SO_2$ was changed *in vitro* not by changing speed but by using gases with different N_2–O_2 gas mixtures (Lindberg and Oberg 1991, Roggan *et al* 1999). Thus, even if $\%SO_2$ oscillations are detectable by the PPG instrumentation (considered negligible by Challoner (1979)), they cannot in any case explain the (positive) pulsations because their contribution is negative. In other words, V-induced $\%SO_2$ changes cannot be the cause of PPG pulsations.

In figure 9(a) is also shown the effect on PPG signal induced by possible positive periodic changes in $\mu_s'(\lambda)$ (figure 9(c)) or $\mu_a(\lambda)$ (figure 9(d)). It is clear from figure 9 that $\mu_s'(\lambda)$ or $\mu_a(\lambda)$ values must increase to reproduce the positive PPG pulsations observed *in vivo*. This means that in the future it will be mandatory to realize new $\mu_s'(\lambda)$ and $\mu_a(\lambda)$ measurements *in vivo* to explain the difference with the *in vitro* data (see introduction).

To this concern, note that Lindberg and Oberg (1991) observed a decrease in the intensity of the transmitted light on whole blood flowing in a rigid glass tube when ranging flow from 0 to 4 ml min^{-1}. After having reached a minimum value at around 4 ml min^{-1}, the intensity started to increase. In practice this means that when going from 0 to 4 ml min^{-1} the $\mu_s'(\lambda)$ and/or $\mu_a(\lambda)$ values must *a fortiori* increase to explain the decreasing intensity and as a consequence the PPG signal increases. Thus, measurements on whole blood (i.e. not plasma free) in the [0, 4] ml min^{-1} interval seem to reproduce the PPG behaviour observed *in vivo*. Interesting enough, the value of 4 ml min^{-1} corresponds to a blood velocity of $\sim$6 mm s^{-1} for the considered experimental setup. An interval of [0, 6] mm s^{-1} may be compatible with the expected range of mean velocity values for PPG visible vessels for a living tissue (Guyton 1991).

In must be noted, that the discrepancy between *in vitro* and *in vivo* data found in the literature was already highlighted and summarized in the past by Roberts (1982). This note also reports the original *in vitro* observation (measurements on a small acrylic tube and simulation with a mathematical model) that there may be preferential diffusion of photons in the direction of blood flow, which then influence the detected PPG signal. It would be interesting to know how this phenomenon *in vivo* would manifest, where the complexity of the vascular network is very high and where the direction of the blood flow is mainly constant inside the vessels.

4.2. Pulse wave velocity in bone vessels

In this study we have seen that it is possible to estimate the arterial Φ-pulse wave velocity also with LDF (mean speed of the pulse wave going from the left heart ventricle to the detection point in bone). This gives similar values to that obtained by means of PPG detectors (Nichols *et al* 2011). Obviously, to improve the precision of this measurements it would be necessary to increase the sensitivity of the LDF, for example, by utilizing many detectors and detector fibres in parallel, which is work for future technical improvements. The important point here is the fact that the detection point was situated in the bone. This means that, in principle, by measuring at different detection points along a long bone (e.g. the tibia), by means of the LDF or PPG technique, one should be able to estimate the speed of propagation of the blood wave *inside* the bone. This new approach may be of great importance in the investigation of a wide variety of pathological skeletal conditions, including trauma, infection, inflammation, arthritis, avascular necrosis neoplasms and bone grafting (Dyke and Aaron 2010).

We hope that this note will contribute to better understand PPG signals, but in particular to further develop the domain of the vascular physiology of human bone.

Acknowledgments

The authors kindly thank Dr Ronald Hogg for the personal sponsoring of the special photodetector for the LDF instrumentation. A special thank you also to Dr Egbert Freiberg (Fietje Sensor&Optoelektronik GmbH, Germany) for the relative spectral emission data for the LED utilized in the simulation. This work has been supported in part (JR, JNH) by the Center for Biomedical Imaging (CIBM) of the Geneva and Lausanne Universities, EPFL, and the Leenaards and Louis-Jeantet Foundations.

References

Allen J 2007 Photoplethysmography and its application in clinical physiological measurement *Physiol. Meas.* **28** R1–39

Aziz S M, Khambatta F, Vaithianathan T, Thomas J C, Clark J M and Marshall R 2010 A near infrared instrument to monitor relative hemoglobin concentrations of human bone tissue *in vitro* and *in vivo* *Rev. Sci. Instrum.* **81** 043111

Binzoni T, Bianchi S, Fasel J H, Bounameaux H, Hiltbrand E and Delpy D T 2002 Human tibia bone marrow blood perfusion by non-invasive near infrared spectroscopy: a new tool for studies on microgravity *J. Grav. Physiol.* **9** P183–4

Binzoni T, Boggett D and Van De Ville D 2011 Laser-Doppler flowmetry at large interoptode spacing in human tibia diaphysis: Monte Carlo simulations and preliminary experimental results *Physiol. Meas.* **32** N33–53

Binzoni T, Leung T, Hollis V, Bianchi S, Fasel J H, Bounameaux H, Hiltbrand E and Delpy D 2003a Human tibia bone marrow: defining a model for the study of haemodynamics as a function of age by near infrared spectroscopy *J. Physiol. Anthropol. Appl. Hum. Sci.* **22** 211–8

Binzoni T, Leung T S, Boggett D and Delpy D 2003b Non-invasive laser Doppler perfusion measurements of large tissue volumes and human skeletal muscle blood RMS velocity *Phys. Med. Biol.* **48** 2527–49

Binzoni T, Leung T S, Courvoisier C, Giust R, Tribillon G, Gharbi T and Delpy D T 2006 Blood volume and haemoglobin oxygen content changes in human bone marrow during orthostatic stress *J. Physiol. Anthropol.* **25** 1–6

Binzoni T and Van De Ville D 2011 Non-invasive probing of the neuro-vascular system in human bone/bone-marrow using near-infrared light *J. Innovative Opt. Health Sci.* **4** 183–9

Brookes M and Revell W J 1998 *Blood Supply of Bone: Scientific Aspects* (London: Springer)

Challoner A V I 1979 *Non-Invasive Physiological Measurements* ed P Rolfe (London: Academic) pp 125–51

Comroe J H 1977 *Physiology of Respiration* (Chicago, IL: Year Book Medical Publisher)

Di Ciccio T J and Efron B 1996 Bootstrap confidence intervals *Stat. Sci.* **11** 189–228

Dobbe J G, Hardeman M R, Streekstra G J, Strackee J, Ince C and Grimbergen C A 2002 Analyzing red blood cell-deformability distributions *Blood Cells Mol. Dis.* **28** 373–84

Dyke J P and Aaron R K 2010 Noninvasive methods of measuring bone blood perfusion *Ann. New York Acad. Sci.* **1192** 95–102

Edwards J R, Williams K, Kindblom L G, Meis-Kindblom J M, Hogendoorn P C, Hughes D, Forsyth R G, Jackson D and Athanasou N A 2008 Lymphatics and bone *Hum. Pathol.* **39** 49–55

Farrell T J, Patterson M S and Wilson B 1992 A diffusion theory model of spatially resolved, steady-state diffuse reflectance for the noninvasive determination of tissue optical properties *in vivo* *Med. Phys.* **19** 879–88

Friebel M, Helfmann J, Müller G and Meinke M 2007 Influence of shear rate on the optical properties of human blood in the spectral range 250 to 1100 nm *J. Biomed. Opt.* **12** 054005

Guyton A C 1991 Overview of the circulation and medical physics of pressure, flow, and resistance *Textbook of Medical Physiology* (Philadelphia, PA: Saunders) pp 150–8

Lindberg L G and Oberg P A 1991 Photoplethysmography: part 2. Influence of light source wavelength *Med . Biol. Eng. Comput.* **29** 48–54

Lindberg L G and Öberg P øA 1993 Optical properties of blood in motion *Opt. Eng.* **33** 253–7

Mateus J and Hargens A R 2012 Photoplethysmography for non-invasive *in vivo* measurement of bone hemodynamics *Physiol. Meas.* **33** 1027–4

Mishchenko M I, Hovenier J W and Travis L D (ed) 2000 *Light Scattering by Nonspherical Particles: Theory, Measurements, and Applications* (San Diego, CA: Academic)

Näslund J, Pettersson J, Lundeberg T, Linnarsson D and Lindberg L G 2006 Non-invasive continuous estimation of blood flow changes in human patellar bone *Med. Biol. Eng. Comput.* **44** 501–9

Näslund J, Waldén M and Lindberg L G 2007 Decreased pulsatile blood flow in the patella in patellofemoral pain syndrome *Am. J. Sports Med.* **35** 1668–73

Nichols W W, O'Rourke M F and Vlachopoulos C 2011 *McDonald's Blood Flow in Arteries: Theoretical, Experimental and Clinical Principles* 6th edn (London: Hodder Arnold)

Roberts V C 1982 Photoplethysmography—fundamental aspects of the optical properties of blood in motion *Trans. Inst. Meas. Control* **4** 101–6

Roggan A, Friebel M, Do Rschel K, Hahn A and Muüller G 1999 Optical properties of circulating human blood in the wavelength range 400–2500 nm *J. Biomed. Opt.* **4** 36–46

Solà J, Rimoldi S F and Allemann Y 2010 Ambulatory monitoring of the cardiovascular system: the role of pulse wave velocity *New Developments in Biomedical Engineering* ed D Campolo (Rijeka: InTech) chapter 21

West J B 1990 *Respiratory Physiology* (Baltimore, MD: Williams & Wilkins)